

See discussions, stats, and author profiles for this publication at: <https://www.researchgate.net/publication/10583715>

Determination of bilayer thickness and lipid surface area in unilamellar dimyristoylphosphatidylcholine vesicles from small-angle neutron scattering curves: A comparison of evaluat...

ARTICLE in EUROPEAN BIOPHYSICS JOURNAL · JULY 2004

Impact Factor: 2.22 · DOI: 10.1007/s00249-003-0349-0 · Source: PubMed

CITATIONS

82

READS

57

3 AUTHORS:



Norbert Kucerka

National Research Council Canada

78 PUBLICATIONS 2,679 CITATIONS

SEE PROFILE



Mikhail Alekseyevich Kiselev

Joint Institute for Nuclear Research

63 PUBLICATIONS 1,211 CITATIONS

SEE PROFILE



Pavol Balgavý

Comenius University in Bratislava

165 PUBLICATIONS 1,556 CITATIONS

SEE PROFILE

Norbert Kučerka · Mikhail A. Kiselev · Pavol Balgavý

Determination of bilayer thickness and lipid surface area in unilamellar dimyristoylphosphatidylcholine vesicles from small-angle neutron scattering curves: a comparison of evaluation methods

Received: 28 October 2002 / Revised: 19 July 2003 / Accepted: 19 July 2003 / Published online: 3 September 2003
© EBSA 2003

Abstract Small-angle neutron scattering (SANS) experiments were performed on unilamellar 1,2-dimyristoylphosphatidylcholine (DMPC) vesicles prepared in heavy water by extrusion through polycarbonate filters with 500 Å pores. The data obtained at 30 ± 0.1 °C were evaluated using a five-strip function model of the bilayer coherent neutron scattering length density, three different approximate form factors describing scattering from vesicles, and different methods of evaluation of the experimental data. It is shown that the results obtained from the SANS data in the range of scattering vector values $0.0316 \text{ Å}^{-1} < q < 0.0775 \text{ Å}^{-1}$ are not sensitive to the vesicle form factor, nor to the evaluation method. Using the hollow sphere model of vesicles convoluted with the Gaussian distribution of their sizes, a constrained bilayer polar region thickness of 9 Å and a DMPC headgroup volume of 325.5 Å^3 , it was possible to obtain from the experimental data the DMPC surface area as $58.9 \pm 0.8 \text{ Å}^2$, the bilayer thickness as $44.5 \pm 0.3 \text{ Å}$ and the number of water molecules as 6.8 ± 0.2 per DMPC located in the bilayer polar region.

Keywords Bilayer thickness · 1,2-Dimyristoylphosphatidylcholine · Lipid surface area · Small-angle neutron scattering · Unilamellar vesicles

Introduction

Two major components of biological membranes are lipids and proteins. Integral membrane proteins, which span the lipid bilayer, mediate the transport of matter and signals. It is well known that the function and properties of many of these proteins depend on the lipid bilayer thickness. Therefore, to have a clear understanding of the factors responsible for various membrane properties, an investigation of lipid bilayer thickness is necessary. The bilayer thickness is studied in model membrane systems (lamellar phospholipid phases, multilamellar and unilamellar phospholipid vesicles) using mainly small-angle X-ray diffraction and scattering methods (see Nagle and Tristram-Nagle 2000; Kiselev et al. 2003 for recent references). Small-angle neutron scattering (SANS) on unilamellar vesicles has not been used in this field so frequently until recently.

In the present paper we study the bilayer thickness, d_L , and the lipid surface area, A_L , at the bilayer/aqueous phase interface in unilamellar 1,2-dimyristoylphosphatidylcholine (DMPC) vesicles using SANS. Although the scattering problem is solved and the scattering theory very well known (Glatter and Kratky 1982; Feigin and Svergun 1987), it is necessary to assume different approximations and models in the evaluation of experimental SANS data. The most frequently used constraint is the homogenous coherent neutron scattering length density, ρ , within the bilayer: the “top-hat” model (see Knoll et al. 1981; Komura et al. 1982; Nawroth et al. 1989; Gordeliy et al. 1993; Balgavý et al. 1998; Gilbert et al. 1999; Mason et al. 1999; Pencer and Hallett 2000; Uhríková et al. 2000 and references therein). However, fully hydrated lipid bilayers include some amount of water inside the lipid polar headgroup region of the bilayer and ρ is not homogeneous within

N. Kučerka (✉)
Department of Chemical Theory of Drugs,
Faculty of Pharmacy,
Comenius University, Kalinčiakova 8, 832 32
Bratislava, Slovakia
E-mail: norbert.kucerka@fpharm.uniba.sk

M. A. Kiselev
Frank Laboratory of Neutron Physics,
Joint Institute for Nuclear Research,
141980 Dubna, Moscow Region, Russia

P. Balgavý
Department of Physical Chemistry,
Faculty of Pharmacy,
Comenius University,
Odbojárov 10, 832 32
Bratislava, Slovakia

the bilayer. These facts have been taken into account in strip function models of the bilayer ρ in recent publications (Balgavý et al. 2001a, 2001b; Schmiedel et al. 2001). In these models, the bilayer was divided into two polar region strips containing a limited number of water molecules besides the lipid headgroup and the hydrophobic region strip ("3"-strip model). Within each strip, ρ was supposed to be homogeneous. Introduction of a strip containing terminal methyl groups of the lipid hydrocarbon chains in the bilayer center and the assumption of a homogeneous ρ within each strip results in the "5"-strip model. The primary aim of the present paper is to obtain the bilayer thickness d_L and the lipid surface area A_L using this "5"-strip model, three different approximate forms of the vesicle form factor, and three different forms for the vesicle size distribution, as well as different methods of fitting the experimental data.

Materials and methods

Sample preparation

Synthetic DMPC was purchased from Sigma (Paris, France). Heavy water (99.98% $^2\text{H}_2\text{O}$) was obtained from Isotop (Moscow, Russia). The heavy water and DMPC were mixed in a plastic tube and the tube was sealed. The DMPC concentration in the sample was 1 wt%. The tube content was heated to a temperature above the main phase transition temperature and then cooled down to about 10 °C. The cooling–heating cycle accompanied by sample shaking was repeated five times. From the dispersion of multilamellar vesicles thus obtained, extruded unilamellar vesicles were prepared in a single-step procedure according to MacDonald et al. (1991) using the LiposoFast Basic extruder (Avestin, Ottawa, Canada). The multilamellar vesicles were extruded through one polycarbonate filter (Nucleopore, Pleasanton, USA) with pores of diameter 500 Å, mounted in the extruder fitted with two gas-tight Hamilton syringes (Hamilton, Reno, USA). The sample was subjected to 25 passes through the filter at a temperature above the main phase transition temperature of the lipid dispersion. An odd number of passes was performed to avoid contamination of the sample by large and multilamellar vesicles, which might not have passed through the filter. The sample was filled into a quartz cell (Hellma, Müllheim, Germany) with a 2 mm sample thickness. The pD of this preparation was about 5. The period between the sample preparation and its measurement was 3–4 h.

SANS measurements

The SANS measurements were performed at the small-angle time-of-flight axially symmetric neutron scattering spectrometer MURN (now named YuMO in honor of the deceased Yu. M. Ostanevich) at the IBR-2 fast pulsed reactor of the Frank Laboratory of Neutron Physics, Joint Institute for Nuclear Research in Dubna (Vagov et al. 1983; Ostanevich 1988). The spectrometer is equipped with circular multiwire proportional ^3He detectors (Ananyev et al. 1978; Ostanevich 1988). The sample temperature was set to 30 °C and controlled electronically with a precision of ± 0.1 °C. The cell with the sample was equilibrated for 1 h at the given temperature in the sample holder before measurement. The neutron scattering cross-section was obtained by using a vanadium standard scatterer as described (Ostanevich 1988). The coherent macroscopic cross-section was calculated from the normalized cross-section according to procedure described by Schmiedel et al. (2001).

Evaluation of SANS data

Scattering theory

The experimentally observed coherent scattering intensity is due to the scattering of neutrons from sample nuclei and the interference of scattered waves. For the monodisperse system it is given by:

$$I(\mathbf{q}) = NP(\mathbf{q})S(\mathbf{q}) \quad (1)$$

where \mathbf{q} is the scattering vector, N is the number of particles, $P(\mathbf{q})$ is the particle structure factor and $S(\mathbf{q})$ is the interparticle structure factor (Glatter and Kratky 1982; Feigin and Svergun 1987). The particle structure factor $P(\mathbf{q})$ is equal to the square of the form factor $F(\mathbf{q})$. In the case of statistically isotropic centrosymmetric particles, one can average through the solid angle (Glatter and Kratky 1982; Feigin and Svergun 1987) to obtain:

$$F(q) = 4\pi \int_0^\infty r^2 \rho(r) \frac{\sin(qr)}{qr} dr \quad (2)$$

This equation can be solved analytically or by using some simplifying assumptions. The analytical solution of the form factor is referred to as the Rayleigh–Gans–Debye formula (RGD). For the q range used in the present paper, the interparticle structure factor $S(\mathbf{q})$ is approximately equal to 1 for dilute and weakly interacting spherical particles, such as the aqueous dispersion of uncharged unilamellar vesicles at a phospholipid concentration of ≤ 1 wt% (Nawroth et al. 1989; Kiselev et al. 2001b).

Vesicle models

Hollow spheres Let us suppose that the unilamellar vesicles are hollow spheres (HS) with the aqueous phase inside and outside the bilayer. In the present paper we suppose that each of the two monolayers in the bilayer consists of three shells. The inner radius of the bilayer is R_0 , and then the radii of the individual shells follow until the outer bilayer radius R_6 . The polar headgroup shell is characterized by the thickness $d_P = R_1 - R_0 = R_6 - R_5$ and the non-polar methylene and methyl groups shells are characterized by thicknesses $d_N = R_2 - R_1 = R_5 - R_4$ and $d_S = R_3 - R_2 = R_4 - R_3$, respectively. The bilayer thickness is then $d_L = 2d_P + 2d_N + 2d_S$. The vesicle structure factor without the background is given by the equations:

$$P_{\text{HS}}(q) = \left(\frac{4\pi}{q^3} \right)^2 \left\{ \sum_{i=1}^6 \Delta\rho_i (A(R_i) - A(R_{i-1})) \right\}^2 \quad (3)$$

$$A(R_i) = qR_i \cos(qR_i) - \sin(qR_i) \quad (4)$$

where $\Delta\rho_i = \rho_w - \rho_i$ are the contrast values of individual strips against the aqueous phase. The polar region strips can contain some amount of water per lipid molecule, N_L , besides the "dry" polar headgroup.

Equations (3) and (4) above are valid for size monodisperse vesicles. The experimentally studied unilamellar vesicles have some degree of radius polydispersity at constant values of the thickness parameters d_P , d_N and d_S . This polydispersity may be described by a Gaussian distribution function of the form:

$$f_G(R) = \frac{1}{\sqrt{2\pi}\sigma_R} \exp \left[-\frac{(R - R_{\text{mean}})^2}{2\sigma_R^2} \right] \quad (5)$$

where R is the outer radius of the vesicles, R_{mean} the mean outer radius of the vesicles, and σ_R the standard deviation of R characterizing the size distribution (Komura et al. 1982). Size polydispersity can also be successfully described by a Schulz distribution function (S) (Hallet et al. 1991; Pedersen et al. 1995), which has the form:

$$f_S(R) = \left(\frac{t+1}{R_{\text{mean}}} \right)^{t+1} \frac{R^t}{\Gamma(t+1)} \exp \left[-\frac{t+1}{R_{\text{mean}}} R \right] \quad (6)$$

where:

$$t = \left(\frac{R_{\text{mean}}}{\sigma_R} \right)^2 - 1 \quad (7)$$

and where $\Gamma(t)$ is the gamma function and $t > 0$. The structure factor of the polydisperse spherical vesicles is obtained by convoluting the single particle $P(q)$ function with the distribution function $f(R)$.

An approximate form of $P(q)$, which includes the effects of vesicle polydispersity, was developed by Moody (1975); we have extended it for the “5”-strip HS model and refer to it as M.

Planar thin sheets

In the case when the radius of the unilamellar liposomes is larger relative to the membrane thickness, the vesicle form factor can be written as a product of the form factor of an infinitively thin sphere and the bilayer form factor (Kiselev et al. 2002). In our case, the form factor of a sphere describes the scattering curve in the range of $q < 0.03 \text{ \AA}^{-1}$ and the form factor of a bilayer describes the scattering curve for $q > 0.03 \text{ \AA}^{-1}$. Thus, to analyze our scattering curve the model of planar thin sheets (PTS) randomly distributed in the aqueous phase can be used. The structure factor without the background of such particles is obtained from the Fourier transformation of the scattering length density of randomly oriented thin sheets. For the “5”-strip model of bilayer, it has the form:

$$P_{\text{PTS}}(q) = \frac{4}{q^4} \left[\sum_{i=1}^3 \Delta\rho_i (\sin(qa_i) - \sin(qa_{i-1})) \right]^2 \quad (8)$$

where the summation goes through one monolayer of bilayer and a_i denote the borders of each monolayer shell.

Contrasts

The values of ρ_i used in the evaluation of the experimental data were calculated using the published neutron scattering lengths for elements (Sears 1986; Munter 1999) and the DMPC component volumes. The molecular volume of DMPC was obtained from the absolute specific volume, $v_L = 0.978 \text{ mL/g}$ at 30°C , measured by a neutral buoyancy method (Petrache et al. 1998) as:

$$V_L = v_L M_w / N_A \quad (9)$$

where M_w is the DMPC molecular weight and N_A is the Avogadro number. To obtain the hydrocarbon region volume, the component volume of the headgroup, V_H , was subtracted from the DMPC molecular volume. It was then supposed that the component volume of the methylene group, V_{CH_2} , is independent of its position in the acyl chain and equals half of the component volume of the methyl group, V_{CH_3} (Nagle and Wilkinson 1978; Nagle et al. 1996; Petrache et al. 1997; Armen et al. 1998). Finally, it was supposed that the volume of the water molecule located in the headgroup region is the same as in the bulk aqueous phase (Wiener et al. 1988; Balgavý et al. 1998) and the data collected in Weast (1969) were used. For the volume of the “dry” headgroup we supposed $V_D = V_H$. The values of V_H in the literature range from 319 \AA^3 to 360 \AA^3 (see Balgavý et al. 2001b for references). The component volumes calculated using these two extreme V_H values are collected in Table 1.

Resolution function

The instrumental resolution can be introduced into the calculation according to Ostanevich (1988) or by convolution of the intrinsic

Table 1 Component volumes of DMPC bilayers at 30°C

$V_L \text{ (\AA}^3\text{)}$	1101	1101
$V_H \text{ (\AA}^3\text{)}$	319	360
$V_{\text{CH}_2} \text{ (\AA}^3\text{)}$	27.929	26.464
$V_{\text{CH}_3} \text{ (\AA}^3\text{)}$	55.858	52.929
$V_{\text{H}_2\text{O}} \text{ (\AA}^3\text{)}$	30.031	30.031
$V_{\text{D}_2\text{O}} \text{ (\AA}^3\text{)}$	30.131	30.131

intensity I_i with a distribution function (Pedersen 1993) which characterizes the deviation in the q value:

$$I_{\text{exp}}(q) = \int G(q') I_i(q') dq' \quad (10)$$

To simplify the evaluation of the experimental data, we approximated the resolution function by a Gaussian function:

$$G(q') = \frac{1}{\sqrt{2\pi}\sigma} \exp \left[-\frac{(q' - q)^2}{2\sigma^2} \right] \quad (11)$$

where σ is the variance of the variable q and depends on q . The value of the second moment of the distribution function, $\sigma(q)$, was calculated for the experimental data as the weighted average over all detector circles. Its value is available for each point of the experimental scattering curve. In the q range used, the mean value of $\sigma(q)/q$ was between 0.05 and 0.07.

Fitting of the experimental data

KP method This method was described and discussed extensively in our recent papers (Balgavý et al. 2001a, 2001b). It is supposed that the scattering curve can be exponentially approximated in the selected range of small q values by:

$$I(q) = I(0)q^{-2} \exp(-R_i^2 q^2); \quad R_i q < 1 \quad (12)$$

where $I(0)$ and R_i are constants. Recall that this approximation is generally referred to as the Guinier approximation. In the present paper, we use the range $q^2 \in (0.001; 0.006) \text{ \AA}^{-2}$. In this range, the experimental value of R_i , $R_i(\text{exp})$, is obtained from the Kratky–Porod (KP) plot ($\ln[I(q)q^2]$ versus q^2) of the experimental SANS curve by a linear fitting procedure (see Fig. 1, Table 2). Then a computer simulated SANS curve is calculated using the HS or PTS model of the vesicles and of the “5”-strip model of the coherent scattering length density distribution in the bilayer. In the calculation, the input values are the volumes V_i of different parts of the bilayer and the values of their coherent scattering amplitudes, b_i . In the first step, the number of water molecules per one DMPC molecule located in the bilayer polar region, N_L , is fixed to one value from the interval $N_L \in (0; 10)$ and the lipid surface area A_L to some starting values A_L^0 and A_L^1 from the interval $A_L \in (40; 80) \text{ \AA}^2$. Then the contrasts are calculated as described above. In the case of the HS model, the polydispersity of vesicle sizes is taken into account either by convoluting the single particle scattering function, $P(q)$, with one of the distribution functions, $f(R)$, or using the approximate form of $P(q)$ developed by Moody (1975). When convoluting with the Gaussian function, the values of $R_{\text{mean}} = 300 \text{ \AA}$ and $\sigma_R = 91 \text{ \AA}$ were used. They were calculated from experimental data in Balgavý et al. (1998). For convolution with the Schulzian function, the values of $R_{\text{mean}} = 260 \text{ \AA}$ and $t = 8$ obtained for extruded DMPC vesicles in Kiselev et al. (2001a) were adopted. For both models (HS and PTS), the calculated SANS curves are convoluted by the resolution function of Eqn. (11). Finally, the values of R_i^2 , $R_i^2(A_L^0)$ and $R_i^2(A_L^1)$ are obtained from the simulated SANS curves by the linear fitting procedure and compared with $R_i^2(\text{exp})$. The starting values of A_L are chosen to fulfill the condition $R_i^2(A_L^1) < R_i^2(\text{exp}) < R_i^2(A_L^0)$. Then this procedure is cycled by changing A_L^{i-1} and A_L^i pairs fulfilling the condition $R_i^2(A_L^i) < R_i^2(\text{exp}) < R_i^2(A_L^{i-1})$ for the given N_L until $|A_L(i) - A_L(i-1)| \leq 0.001 \text{ \AA}^2$. In the following steps, N_L is

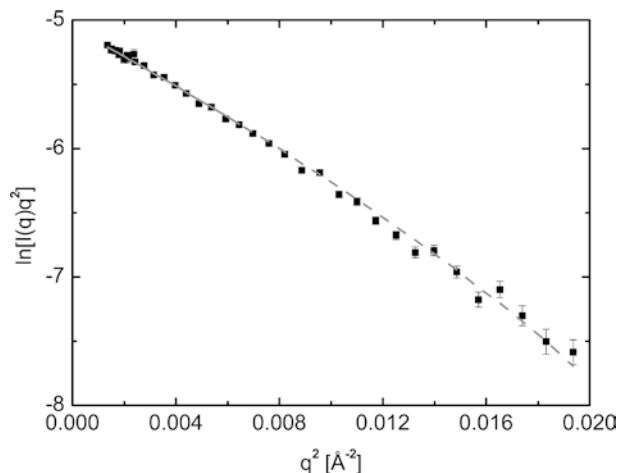


Fig. 1 Kratky-Porod plot of experimental SANS data. *Full curve*: linear fit to experimental points; *dashed curve*: calculated using the HS + KP results in Table 2. In the q range where the fit was done, the full and dashed curves overlap

fixed to other values from the interval $N_L \in (0; 10)$ and for each value of N_L the cycle described above is repeated. The result is a set of A_L values as a function of N_L . Since the volumetric data are known, the bilayer thickness d_L is calculated from A_L as well.

MKP method Pencer and Hallet (2000) proposed a modified Kratky-Porod (MKP) method based on finding the position of the first local maximum in the $I(q)q^4$ versus q plot, q_{\max} . This method follows the theoretical law of asymptotic behavior of a scattering curve. From the value of q_{\max} they have obtained the bilayer thickness in unilamellar liposomes, supposing a homogeneous distribution of coherent neutron scattering length density within the bilayer. We have extended their approach using the “5”-strip model of the bilayer and the HS and PTS models of the vesicles. The experimental $I(q)q^4$ versus q data were fitted with a polynomial in the range $q \in (0.035; 0.102) \text{ \AA}^{-1}$ to obtain the position $q_{\max}(\text{exp})$ of the $I(q)q^4$ maximum. Then the simulated curves were calculated as described above for pairs of $A_L(i)$ and $A_L(i-1)$ and the values of $q_{\max}(A_L^i)$ and $q_{\max}(A_L^{i-1})$ were obtained from the simulated curves. The conditions $q_{\max}(A_L^i) < q_{\max}(\text{exp}) < q_{\max}(A_L^{i-1})$ and $|A_L(i) - A_L(i-1)| \leq 0.001 \text{ \AA}^2$ are used to obtain the value of A_L for the given N_L . The result is a set of paired A_L and N_L values as above.

Results and discussion

The experimental SANS data are shown in Figs. 1 and 2 using the KP and MKP plots, respectively. The scatter of

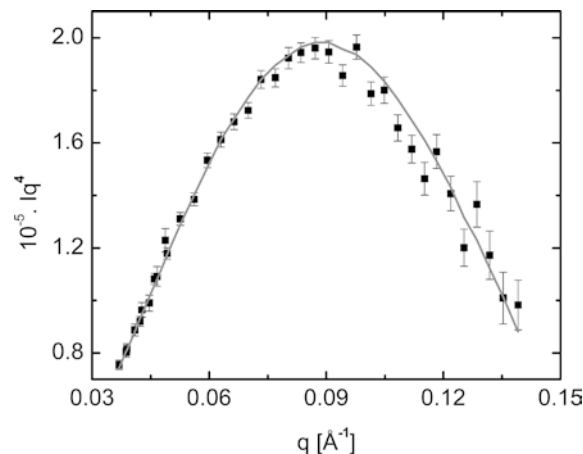


Fig. 2 Modified Kratky-Porod plot of experimental SANS data. *Full curve* is the best fit calculated using the HS + MKP results in Table 2

the experimental points and their uncertainty (error bars) increase with the increase of q . This is due to the reduction of SANS with the increase of scattering angle. The full line in the KP plot was obtained by a linear fit of the experimental data in the range $q^2 \in (0.001; 0.006) \text{ \AA}^{-2}$. The slope parameter, $R_L^2(\text{exp}) = 122.04 \pm 2.88 \text{ \AA}^2$, obtained from the KP plot, and the maximum parameter, $q_{\max}(\text{exp}) = 0.0896 \pm 0.0057$, obtained from the MKP plot, were then used to obtain paired values of d_L (A_L) and N_L as described above.

Since the KP and MKP methods are based on extracting one parameter from a linear approximation or local maximum, they reduce the experimental scattering curve to one equation. It is evident that one can exactly solve only the system with one unknown parameter in this case. The frequently used “top-hat” model of the bilayer is characterized just by one parameter, the bilayer thickness, so it can be directly obtained using these methods. However, more realistic models of phospholipid bilayer with several shells and with some amount of water molecules penetrating into the polar headgroup region include several unknown parameters. We have reduced their number to two by taking the lipid component volumes from volumetric data, and the size distribution function and the mean radius of vesicles from another independent experiment.

Table 2 The results of SANS data evaluation obtained using the $V_H = 319 \text{ \AA}^3$ and $d_P = 9 \text{ \AA}$ constraints

Vesicle model	Evaluation method	ρ_{model}	Polydispersity	N_L	$A_L (\text{\AA}^2)$	$d_L (\text{\AA})$
HS	— ^a	“top-hat”	S	—	—	35.20 ± 0.20
HS	KP	5	G	6.90 ± 0.23	58.55 ± 0.76	44.71 ± 0.35
HS	KP	5	S	6.90 ± 0.23	58.53 ± 0.76	44.72 ± 0.35
HS	KP	5	M	6.85 ± 0.26	58.38 ± 0.85	44.79 ± 0.39
HS	MKP	5	G	6.79 ± 0.91	58.17 ± 3.05	44.89 ± 1.41
HS	MKP	5	S	6.78 ± 0.91	58.15 ± 3.05	44.90 ± 1.41
HS	MKP	5	M	6.76 ± 0.91	58.08 ± 3.04	44.93 ± 1.41
PTS	KP	5	—	6.92 ± 0.23	58.60 ± 0.76	44.69 ± 0.34
PTS	MKP	5	—	6.80 ± 0.91	58.22 ± 3.05	44.86 ± 1.41

^aResult from Kiselev et al. (2001a)

The first data sets were calculated using the component volumes in Table 1, obtained when supposing $V_H = 319 \text{ \AA}^3$ (Sun et al. 1996). As an example, Fig. 3 shows selected paired d_L and N_L values obtained using the KP plot, the PTS model of vesicles and the “5”-strip model of the neutron scattering length density ρ of the bilayer. The value of $R_t(\text{exp})$ in the PTS model of vesicles is equal to the bilayer sheet gyration radius taken perpendicularly to the sheet surface (Glatter and Kratky 1982; Feigin and Svergun 1987). The thickness of the two-dimensional planar sheet d_t can be obtained from its radius of gyration R_t as:

$$d_t^2 \approx 12R_t^2 \quad (13)$$

under the condition $2\pi/S^{0.5} \leq q \leq 1/R_t$, where S is the total area of the sheet (Glatter and Kratky 1982; Feigin and Svergun 1987). Several groups of authors supposed that the PTS model of unilamellar vesicles is a good approximation for SANS in the Guinier range of q , and that the vesicle bilayer thickness could be obtained by analogy to Eq. (13) as $d_L = 12^{0.5}R_t(\text{exp})$ (see Knoll et al. 1981; Nawroth et al. 1989; Gordeliy et al. 1993; Balgavý et al. 1998; Uhríková et al. 2000; Uhríková et al. 2003 and references therein). The dashed line in Fig. 3 shows the bilayer thickness obtained from our data using this approximation. It is evident that this simplified approach underestimates the value of the bilayer thickness, even when supposing that there are no water molecules located in the bilayer polar region. However, this approach is useful when one is interested in relative changes of d_L only and not in its absolute values. We have found that the bilayer thickness obtained by using Eq. (13) in the unilamellar vesicles prepared from a homologous series of 1,2-diacylphosphatidylcholines correlates linearly with the transbilayer distance of phosphate groups evaluated from small-angle X-ray scattering data (Balgavý et al. 2001a).

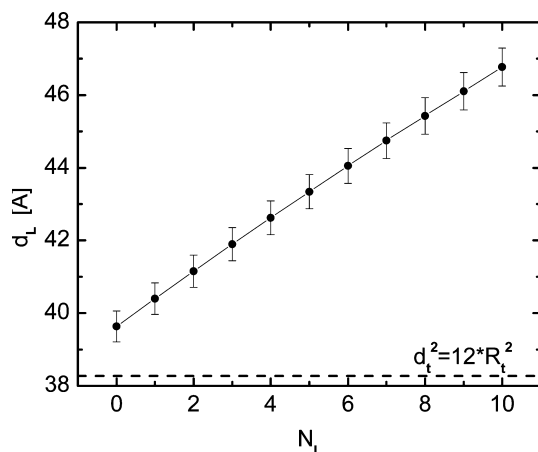


Fig. 3 DMPC bilayer thickness obtained using the PTS model of vesicles, KP method of evaluation and the $V_H = 319 \text{ \AA}^3$ and $d_p = 9 \text{ \AA}$ constraints. Errors propagate from the R_t^2 experimental error

We have calculated the d_L (A_L) versus N_L dependencies as in Fig. 3 for all combinations of vesicle models (HS and PTS) and evaluation methods (KP and MKP). From these dependencies, one can obtain a unique d_L , A_L and N_L combination using complementary information, e.g. from contrast variation (Balgavý et al. 2001a, 2001b), or by using another parametrization of the system. In the present paper we fix the bilayer polar region thickness d_p to a constant $d_p = 9 \text{ \AA}$ obtained from the neutron diffraction data on oriented DPPC multilayers (Büldt et al. 1979; Zaccai et al. 1979). This value is frequently used for obtaining the steric bilayer thickness from X-ray diffraction data (see Nagle and Tristram-Nagle 2000 and references therein). The results obtained by using this procedure are collected in Table 1 and compared with the d_L value obtained for DMPC vesicles when using the “top-hat” model of the bilayer scattering length density (Kiselev et al. 2001a). Several conclusions can be extracted from these data. First, the model of randomly oriented planar thin sheets is equally good as the model of hollow spheres when extracting the d_L , A_L and N_L values from the SANS data obtained with unilamellar vesicles in the q range used. This is what we expected when we reduced the range of q values where the SANS data were evaluated. Second, the form of vesicle size distribution (G =Gauss, S =Schulz, M =Moody) has no effect on the bilayer structural parameters obtained when using the HS model. Third, the Kratky–Porod method yields the same results as the modified Kratky–Porod method when using the mean R_t and q_{max} values. The uncertainty in the obtained results is higher in the modified Kratky–Porod method. This is caused by the lower signal-to-noise ratio in the q value region used to obtain the q_{max} value comparing to the R_t value (see Fig. 2). Finally, the distribution of the scattering length density in the bilayer influences the results of the experimental data evaluation significantly: the “top-hat” model of the bilayer compared to the “5”-strip model underestimates the bilayer thickness d_L . The general conclusion is that while the vesicle form factor, form of the vesicle size distribution and evaluation method do not greatly affect the results of the analysis, the model of the bilayer coherent neutron scattering length density significantly influences the results obtained from the SANS data in the selected region of the scattering vector values.

The critical point in all models of the bilayer coherent neutron scattering length density is the exact value of the phospholipid headgroup volume, V_H ; this value is equally important in the evaluation of bilayer structural parameters from the X-ray diffraction data (Nagle and Tristram-Nagle 2000). As mentioned above, the V_H values for 1,2-diacylphosphatidylcholines used in the literature range from 319 \AA^3 to 360 \AA^3 . To assess the influence of the V_H parameter, we have calculated the dependencies of N_L , d_L and A_L on the V_H value in this range. We have found that the A_L parameter increases from $A_L = 58.6 \pm 0.8 \text{ \AA}^2$ at $V_H = 319 \text{ \AA}^3$ to $A_L = 61.0 \pm 0.8 \text{ \AA}^2$ at $V_H = 360 \text{ \AA}^3$, while the N_L and d_L

parameters are rather insensitive to the V_H change, moving from $N_L = 6.9 \pm 0.2$ and $d_L = 44.7 \pm 0.4 \text{ \AA}$ at $V_H = 319 \text{ \AA}^3$ to $N_L = 6.3 \pm 0.2$ and $d_L = 43.6 \pm 0.3 \text{ \AA}$ at $V_H = 360 \text{ \AA}^3$. Petrache et al. (1998) used the modified Caillé theory for the interpretation of synchrotron X-ray diffraction on multilamellar DMPC vesicles and the $V_H = 319 \text{ \AA}^3$ value as we used above. They incubated DMPC in aqueous solutions containing various amounts of polyvinylpyrrolidone, varying the osmotic pressure and, consequently, the bilayer hydration. They obtained the DMPC surface area as $A_L = 59.7 \pm 0.2 \text{ \AA}^2$ for the fully hydrated DMPC at 30°C by extrapolating the A_L value to zero osmotic pressure using the elastic area compressibility modulus of DMPC and $V_H = 319 \text{ \AA}^3$. Taking into account the experimental errors, one could conclude that the surface areas of DMPC obtained in unilamellar and multilamellar vesicles at full hydration by SANS and by diffraction, respectively, are very close. The value of $V_H = 319 \text{ \AA}^3$ used above has been the most reliable experimental value until recently. It was calculated from the simultaneous evaluation of small- and wide-angle X-ray diffraction data obtained with the fully hydrated lamellar L_β' gel phase of DPPC (Sun et al. 1994). It has been suggested to be the same in the fully hydrated fluid lamellar DPPC phase, as well as in bilayers from lipids having the same phosphatidylcholine headgroup (Nagle and Tristram-Nagle 2000). However, a significantly higher value of $V_H = 331 \text{ \AA}^3$ was obtained by simultaneous evaluation of the small- and wide-angle diffraction data obtained with the DMPC lamellar gel phase (Tristram-Nagle et al. 2002). Using this latter number of V_H instead of the former changes the surface area value for the DMPC in unilamellar vesicles to $A_L = 59.3 \pm 0.8 \text{ \AA}^2$ (when using the “5”-strip model of the bilayer, the HS model of the vesicles, the G distribution of their sizes and the KP evaluation method) and in the lamellar fluid phase of DMPC to $A_L = 58.7 \pm 0.2 \text{ \AA}^2$ (J. Nagle, personal communication). The A_L value obtained from SANS increases with V_H , the A_L calculated from X-ray diffraction data decreases with V_H , and our estimate of experimental uncertainty of V_H is about $\pm 5\text{--}6 \text{ \AA}^3$. All the available data for DMPC will match then within experimental error at $V_H = 325\text{--}326 \text{ \AA}^3$, i.e. at a V_H value estimated for egg yolk phosphatidylcholine from the crystallographic data of lipid polar headgroup fragments (Small 1967).

Though the primary aim of our paper was the comparison of different models and evaluation methods used in SANS on unilamellar vesicles, a comparison of our results with the results obtained by other authors has narrowed the V_H interval used for the evaluation of SANS and X-ray diffraction data. We have shown that when using an appropriate bilayer model, structural information could be extracted from the low-resolution SANS data. An obvious drawback of the data analysis in the present paper is the use of the polar region thickness d_p constraint. This constraint can be avoided, e.g. by the simultaneous

evaluation of the data from SANS and from small-angle X-ray scattering on unilamellar vesicles (Balgavý et al. 2001a) and/or by using the SANS data obtained at different contrasts (Balgavý et al. 2001b). The second type of improvement in the SANS data evaluation could be a modification of the strip function models of the coherent neutron scattering density with diffuse strip borders. Finally, the distribution of the scattering length density in the bilayer could be modeled by, for example, several Gaussian functions like the electron density in recent X-ray diffraction studies (see Nagle and Tristram-Nagle 2000; Pabst et al. 2000 for references). We plan to test these SANS data evaluation improvements in future.

Acknowledgements N.K. and P.B. thank the staff of the Condensed Matter Division, Frank Laboratory of Neutron Physics, Joint Institute for Nuclear Research in Dubna, Russia for hospitality, M.K. thanks the Laboratory of Biophysics, Department of Physical Chemistry, Faculty of Pharmacy, Comenius University in Bratislava, Slovakia, for financial support and hospitality. The authors thank Prof. John F. Nagle for discussions at several stages of this work, Dr. Jeremy Pencer for critical reading of the manuscript of this paper and for helpful comments, and Prof. Stanislav Dubnička for generous support and encouragement. This study was supported by the Slovak Ministry of Education VEGA grants 1/7704/2000 and 1/0123/2003 to P.B. and by the Comenius University grants UK/2/2001 and UK/13/2002 to N.K. The experiments in Dubna were supported within the JINR project 07-4-1031-99/03 “Investigation of the structure and dynamics of condensed matter with neutrons”.

References

- Ananyev BN, Kunchenko AB, Lazin VI, Pikelner EYa (1978) An annular multiwire detector of slow neutrons with helium-3. *JINR Commun* 3-11502
- Armen RS, Uitto OD, Feller SE (1998) Phospholipid component volumes: determination and application to bilayer structure calculations. *Biophys J* 75:734–744
- Balgavý P, Dubničková M, Uhríková D, Yaradaikin S, Kiselev M, Gordeliy V (1998) Bilayer thickness in unilamellar extruded egg yolk phosphatidylcholine liposomes: a small-angle neutron scattering study. *Acta Phys Slovaca* 48:509–533
- Balgavý P, Dubničková M, Kučerka N, Kiselev MA (2001a) Bilayer thickness and lipid interface area in unilamellar extruded 1,2-diacylphosphatidylcholine liposomes: a small-angle neutron scattering study. *Biochim Biophys Acta* 1512:40–52
- Balgavý P, Kučerka N, Gordeliy VI, Cherezov VG (2001b) Evaluation of small-angle neutron scattering curves of unilamellar phosphatidylcholine liposomes using a multishell model of bilayer neutron scattering length density. *Acta Phys Slovaca* 51:53–68
- Büldt G, Gally HU, Seelig J, Zaccai G (1979) Neutron diffraction studies on phosphatidylcholine model membranes. I. Head group conformation. *J Mol Biol* 134:673–691
- Feigin LA, Svergun DI (1987) Structure analysis by small-angle X-ray and neutron scattering. Plenum, New York
- Gilbert RJ, Heenan RK, Timmins PA, Gingles NA, Mitchell TJ, Rowe AJ, Rossjohn J, Parker MW, Andrew PW, Byron O (1999) Studies on the structure and mechanism of a bacteria I protein toxin by analytical ultracentrifugation and small-angle neutron scattering. *J Mol Biol* 293:1145–1160
- Glatter O, Kratky O (1982) Small angle X-ray scattering. Academic Press, New York

- Gordeliy VI, Golubchikova LV, Kuklin A, Strykh AG, Watts A (1993) The study of single biological and model membranes via small angle neutron scattering. *Prog Colloid Polym Sci* 93:252–257
- Hallet FR, Nickel B, Samuels C, Krygsman PH (1991) Determination of vesicle size distributions by freeze-fracture electron microscopy. *J Electron Microsc Techn* 17:459–465
- Kiselev MA, Lesieur P, Kisselev AM, Lombardo D, Killany M, Lesieur S (2001a) Sucrose solutions as perspective medium to study the vesicle structure: SAXS and SANS study. *J Alloys Compd* 328:71–76
- Kiselev MA, Lombardo D, Kisselev AM, Lesieur P (2001b) Structure factor of DMPC unilamellar vesicles: SAXS study at synchrotron. *FLNP Annual Report 2000, JINR, Dubna*, pp 136–138
- Kiselev MA, Lesieur P, Kisselev AM, Lombardo D, Aksenov VL (2002) Model of separated form factors for unilamellar vesicles. *Appl Phys A* 74: S1654–S1656
- Kiselev MA, Wartewig S, Janich M, Lesieur P, Kisselev AM, Ollivon M, Neubert R (2003) Does sucrose influence the properties of DMPC vesicles? *Chem Phys Lipids* 123:31–44
- Knoll W, Haas J, Stuhmann HB, Fuldner HH, Vogel H, Sackmann E (1981) Small-angle neutron scattering of aqueous dispersions of lipids and lipid mixtures. *J Appl Crystallogr* 14:191–202
- Komura S, Toyoshima Y, Takeda T (1982) Neutron small-angle scattering from single walled liposomes of egg phosphatidylcholine. *Jpn J Appl Phys* 21:1370–1372
- MacDonald RC, MacDonald RI, Menco BP, Takeshita K, Subbarao NK, Hu LR (1991) Small-volume extrusion apparatus for preparation of large, unilamellar vesicles. *Biochim Biophys Acta* 1061:297–303
- Mason PC, Gaulin BD, Epanand RM, Wignall GD, Lin JS (1999) Small angle neutron scattering and calorimetric studies of large unilamellar vesicles of the phospholipid dipalmitoylphosphatidylcholine. *Phys Rev E* 59:3361–3366
- Moody MF (1975) Diffraction by dispersions of spherical membrane vesicles. I. The basic equations. *Acta Crystallogr A* 31:8–15
- Munter A (2002) Neutron scattering lengths and cross sections. <http://www.ncnr.nist.gov/resources/n-lengths/list.html>
- Nagle JF, Tristram-Nagle S (2000) Structure of lipid bilayers. *Biochim Biophys Acta* 1469:159–195
- Nagle JF, Wilkinson DA (1978) Lecithin bilayers. Density measurement and molecular interactions. *Biophys J* 23:159–175
- Nagle JF, Zhang R, Tristram-Nagle S, Sun W, Petrache HI, Suter RM (1996) X-ray structure determination of fully hydrated L α phase dipalmitoylphosphatidylcholine bilayers. *Biophys J* 70:1419–1431
- Nawroth T, Conrad H, Dose K (1989) Neutron small angle scattering of liposomes in the presence of detergents. *Physica B* 156–157:477–480
- Ostanevich YuM (1988) Time-of-flight small-angle scattering spectrometers on pulsed neutron sources. *Makromol Chem Macromol Symp* 15:91–103
- Pabst G, Rappolt M, Amenitsch H, Laggner P (2000) Structural information from multilamellar liposomes at full hydration: full q -range fitting with high quality x-ray data. *Phys Rev E* 62:4000–4009
- Pedersen JS (1993) Resolution effects and analysis of small-angle neutron-scattering data. *J Phys IV* 3:491–498
- Pedersen JS, Egelhaaf SU, Schurtenberger P (1995) Formation of polymer-like mixed micelles and vesicles in lecithin–bile salt solutions: a small-angle neutron-scattering study. *J Phys Chem* 99:1299–1305
- Pencer J, Hallett FR (2000) Small-angle neutron scattering from large unilamellar vesicles: an improved method for membrane thickness determination. *Phys Rev E* 61:3003–3008
- Petrache HI, Feller SE, Nagle JF (1997) Determination of component volumes of lipid bilayers from simulations. *Biophys J* 72:2237–2242
- Petrache HI, Tristram-Nagle S, Nagle JF (1998) Fluid phase structure of EPC and DMPC bilayers. *Chem Phys Lipids* 95:83–94
- Schmiedel H, Jörchel P, Kiselev M, Klose G (2001) Determination of structural parameters and hydration of unilamellar POPC/C12E4 vesicles at high water excess from neutron scattering curves using a novel method of evaluation. *J Phys Chem B* 105:111–117
- Sears VF (1986) Neutron scattering lengths and cross-sections. In: Skold K, Price DL (eds) *Methods in experimental physics*, vol 23. Academic Press, New York, pp 521–550
- Small DM (1967) Phase equilibria and structure of dry and hydrated egg lecithin. *J Lipid Res* 8:551–557
- Sun WJ, Suter RM, Knewtson MA, Worthington CR, Nagle ST, Zhang R, Nagle JF (1994) Order and disorder in fully hydrated unoriented bilayers of gel phase DPPC. *Phys Rev E* 49:4665–4676
- Sun WJ, Tristram-Nagle S, Suter RM, Nagle JF (1996) Structure of gel phase saturated lecithin bilayers: temperature and chain length dependence. *Biophys J* 71:885–891
- Tristram-Nagle S, Liu Y, Legleiter J, Nagle JF (2002) Structure of gel phase DMPC determined by X-ray diffraction. *Biophys J* 83:3324–3335
- Uhríková D, Balgavý P, Kučerka N, Islamov A, Gordeliy V, Kuklin A (2000) Small-angle neutron scattering study of the n -decane effect on extruded unilamellar dioleoylphosphatidylcholine liposomes. *Biophys Chem* 88:165–170
- Uhríková D, Kučerka N, Islamov A, Kuklin A, Gordeliy V, Balgavý P (2003) Small-angle neutron scattering study of the lipid bilayer thickness in unilamellar dioleoylphosphatidylcholine vesicles prepared by the cholate dilution method: n -decane effect. *Biochim Biophys Acta* 1611:31–34
- Vagov VA, Kunchenko AB, Ostanevich YuM, Salamatina IM (1983) Time-of-flight small-angle neutron scattering spectrometer at pulsed reactor IBR-2. *JINR Commun* P14-83-898
- Weast RC (ed) (1969) *Handbook of chemistry and physics*. Chemical Rubber Co., Cleveland, pp F-4, F-5
- Wiener MC, Tristram-Nagle S, Wilkinson DA, Campbell LE, Nagle JF (1988) Specific volumes of lipids in fully hydrated bilayer dispersions. *Biochim Biophys Acta* 938:135–142
- Zaccai G, Büldt G, Seelig A, Seelig J (1979) Neutron diffraction studies on phosphatidylcholine model membranes. II. Chain conformation and segmental disorder. *J Mol Biol* 134:693–706